Target Journal: *Estuarine, Coastal and Shelf Science*

Application of the extractable lipofuscin aging method to estimate mortality and population dynamics of the burrowing shrimp, *Neotrypaea californiensis*

Running Title: lipofuscin-based mortality estimation

*Katelyn M Bosley[1], Thomas Wainwright[2], Brett R Dumbauld[3]

[1] Department of Fisheries and Wildlife, Oregon State University, Hatfield Marine Science Center, 2030 SE Marine Science Dr., Newport, Oregon, 97365, USA, katelyn.bosley@noaa.gov

[2] Northwest Fisheries Science Center, National Marine Fisheries Service, National Oceanic and Atmospheric Administration (Retired†), 2032 SE OSU Drive, Newport, Oregon 97365, tcwainw@gmail.com

[3] US Department of Agriculture, ARS, Newport, Oregon, 97365, USA, brett.dumbauld@ ars.usda.gov

Current address: Northwest Fisheries Science Center, NMFS-NOAA, 2032 SE OSU Drive, Newport, Oregon 97365

†*Disclaimer*: The views expressed in this article are those of the author and do not reflect the position or policy of the National Oceanic and Atmospheric Administration or the United States government.

ABSTRACT

Lack of robust aging methods for crustaceans has inhibited the use of age-structured population models. Individuals are often classified based on body size, but differences in growth can bias parameter estimates. Our study applied the lipofuscin aging method combined with catch-curve analysis to estimate mortality rate for the burrowing shrimp, *Neotrypaea californiensis*. This species is an important member of the estuarine community with an impact on oyster production along the US West Coast. Randomized surveys were conducted from 2011-2014 to estimate population abundance, average density, and age structure in Yaquina Bay, Oregon. Mortality rate was estimated to be 0.719 yr^{-1} (95% CI; 0.633-0.793 yr^{-1}) and did not vary significantly across cohorts. The spatial extent of the survey revealed spatial patterns in shrimp density that could be explained by variation in mortality and recruitment rates. This is the first study to apply lipofuscin aging to estimate population parameters of an estuarine crustacean and the methods we present can inform managers seeking to incorporate population ecology into management plans for *N. californiensis* and other crustacean species worldwide.

Keywords: lipofuscin; aging; population dynamics; burrowing shrimp; mortality; simulation model

1. INTRODUCTION

Age- and stage-structured population models are among the most widely applied models in population ecology. Introduced by P.H. Leslie (1945), this class of model typically assumes that individuals can be lumped into discrete classes (i.e., age or stage) and that time can be divided into discrete intervals. The inability to accurately determine age in crustaceans due to the lack of hard bony structures in these invertebrates has posed a major problem for researchers and managers attempting to apply age-structured models to estimate vital rates of ecologically or economically important species. Most population models for crustaceans have been length-based or stage-based models where size-transition probabilities are estimated from laboratory experiments or tag-and-release studies (Feinberg et al., 2006; Nilssen and Sundet, 2006; Chang et al., 2012; Ohman, 2012; Punt et al., 2014). However, growth rates among individuals vary greatly depending on environmental conditions (Oh and Hartnoll, 2000; Hartnoll 2001; Stoner et al., 2013) causing overlap in size classes within and among cohorts, ultimately making the relationship between time and size unreliable. Recent studies validating the biochemically-based lipofuscin aging method have shown promise for its use as an alternative to traditional size-based metrics (Vila et al., 2000; Allain et al., 2011; Bluhm and Brey, 2001; Kodama et al., 2006; Puckett et al., 2008). The ability to estimate individual age creates the opportunity to apply classic age-structured models to investigate crustacean population dynamics.

The burrowing shrimp, *Neotrypaea californiensis,* inhabits soft intertidal sediments in estuaries along the US Pacific Northwest coast. Burrowing shrimps are an important component of the estuarine benthic community and play a role in estuarine ecosystem resiliency (Berkenbusch and Rowden, 2003; Berkenbusch and Rowden, 2006; DeWitt et al., 2004; Berkenbusch et al., 2007; D'Andrea and Dewitt, 2009). Pacific Northwest estuaries also support

58 a multimillion-dollar commercial shellfish aquaculture industry (USDA Census of Aquaculture,
59 2012; Northern Economics 2013). Oysters (primarily *Crassostrea gigas*) are often placed
60 directly on the sediment surface of intertidal mudflats to grow (Feldman et al., 2000; Dumbauld
61 et al., 2006). This method subjects newly planted oysters, known as "seed", to the threat of burial
62 through bioturbation by *N. californiensis,* which can result in significant economic losses to
63 growers (Feldman et al., 2000). The presence of burrowing shrimp pests on oysters beds are a
64 concern to growers that operate on grounds overlapping with burrowing shrimp populations
65 (Feldman et al., 2000; Chew, 2002; Dumbauld et al., 2006) and for over 50 years the aquaculture
66 industry had applied topical pesticides to intertidal mudflats to control shrimp populations in
67 oyster beds (WDFW 1970; Feldman et al., 2000). After increasing environmental concerns over
68 the impacts associated with application of the pesticide, carbaryl (WDFW and WDOE, 1992),
69 the shellfish industry in Washington State agreed to transition to integrated pest management
70 (IPM) as part of an effort to improve control while minimizing environmental impacts
71 (Dumbauld et al., 2006).

72 While the industry is still examining alternative pest control measures, including a less
73 toxic pesticide, successful implementation of an IPM plan requires methods to accurately assess
74 burrowing shrimp populations and the development of population models (DeWitt et al., 1997;
75 Dumbauld et al., 2006; Bosley and Dumbauld 2011). Previous researchers have examined the
76 life-history aspects of *N. californiensis*, describing details on growth, fecundity and population
77 age structure which could be used in developing a population model (Bird, 1982; Dumbauld et
78 al., 1996; Bosley and Dumbauld, 2011). Results indicated growth rate varied spatially among
79 populations and though the mechanism is still unclear, Bosley and Dumbauld (2011) showed that
80 growth can vary significantly even within a cohort at a given location. Using the biochemically-

based lipofuscin-based aging method, Bosley and Dumbauld (2011) also demonstrated that *N. californiensis* might have a lifespan of 13 years, more than twice the previous estimate (Bird, 1982; Dumbauld et al., 1996). In light of this new information regarding age and growth in *N. californiensis*, it is clear that estimating population parameters from size-frequency data would produce inaccurate parameter estimates that may not reflect the true population dynamics of the species.

Lipofuscin-based aging methods can overcome the challenges associated with traditional sized-based methods of age determination for *N. californiensis* (e.g. spatial and temporal growth variability). To date, most lipofuscin studies have involved validation of the methodology (Vila et al., 2000; Bluhm and Brey, 2001; Kodama et al., 2006; Puckett et al., 2008; Allain et al., 2011) and a few have used the methods to conduct demographic assessments (Bluhm et al., 2001; Ju et al., 2001; Harvey et al., 2010; Bosley and Dumbauld, 2011). While these studies have provided details regarding growth and life history for several crustacean species, none has extended application of the method to the estimation of population vital rates or development of a population dynamics model, which could be used as part of a management framework.

The ability to predict population-level changes has become the basis for management of biological resources and fisheries and wildlife conservation (Hilborn and Walters, 1992; Udevitz and Ballachey, 1998; Beissinger and McCullough, 2002; Morris and Doak, 2002). Population abundance can be described by the balance between recruitment and mortality rates (Caswell, 2001) and, given robust estimates, these rates can be used to forecast future population sizes. Burrowing shrimp have pelagic larvae that disperse in the coastal ocean and therefore recruitment of *N. californiensis* to estuaries is likely linked to the oceanic environment and could be less predictable than for other species (Dumbauld et al., 1996; Tamaki et al., 2010; Dumbauld

and Bosley, 2018). The sedentary lifestyle of the shrimp, however, allows the adult population to be readily sampled. With the availability of robust aging methods, application of age-based models can be applied to estimate demographic parameters for adult populations of *N. californiensis*.

The goal of our study was to apply the lipofuscin aging method to estimate natural mortality rates for *N. californiensis* populations in Yaquina Bay, Oregon, using a cohort-based approach. The objectives were to 1) conduct annual population assessments of *N. californiensis* in Yaquina Bay, Oregon, USA 2) apply lipofuscin-based aging methods to determine age structure and estimate age-specific mortality rate for the measured population, and 3) construct a cohort-based simulation model that can be used to predict changes in Yaquina Bay shrimp populations under different recruitment and mortality scenarios relevant to their ecology and management. This study represents the first application of lipofuscin aging to understand the population dynamics of a crustacean on the US west coast. In addition, the methodology developed in this study can be used to estimate mortalities for *N. californiensis* populations in other estuaries and provides a tool that can be used in the development of successful management plans for burrowing shrimp in the Pacific Northwest and potentially for other crustacean species worldwide.

2. MATERIALS AND METHODS

2.1 Study site

We sampled a subset of the total population of *N. californiensis* located from the Idaho Flats intertidal mudflat in Yaquina Bay, Oregon, USA (44°37'8.4"N, 124° 2'27.2"W; approx. 16 hectares) located on the central Oregon coast (Fig. 1). Population densities can reach up to 500

127 shrimp m^{-2} in some areas of the bay (DeWitt et al., 2004) and the shrimp can be found at tidal
128 elevations ranging from approximately -2.0 meters relative to mean lower low water (MLLW) to
129 about +3 meters MLLW (AF D'Andrea, unpubl. data, Oregon Department of Fish and Wildlife).
130 We sampled an established population of *N. californiensis* located in the upper intertidal (+2 to
131 +3 meters MLLW) that represents about half of the total population on Idaho Flats (Fig. 1). The
132 survey encompassed a range of densities and was concentrated on a subset of the population on
133 Idaho Flats, allowing greater sampling effort to be made in order to achieve greater precision in
134 population parameter estimates.
135
136 **2.2 Sample collection**
137 Total abundance of *N. californiensis* in the area we sampled was estimated from annual
138 population surveys conducted from 2011 to 2014. Surveys were conducting in July or August
139 each year within a 2-week period. This was done to ensure that samples represented the same
140 temporal period and were comparable across sample years. The spatial extent of the population
141 each year was determined by mapping population bed edges defined by walking along the
142 population edge with a high precision Trimble GeoXT GPS[1]. In areas where a clear bed edge
143 was not visible, bed edges were defined by walking within a zone where burrows were clearly
144 increasing in density to one side and decreasing on the other. This boundary was well defined
145 and usually encompassed a 3-meter distance. Bed edge data were imported into Trimble GPS
146 Pathfinder Office v. 4.20 (Trimble Inc., Sunnyvale, CA) for differential correction and exported
147 as an ERSI shapefile. The spatial bed edge data was then converted into spatial polygons using

1 Use of trade names throughout this publication does not imply endorsement by the U.S. government.

148 'rgdal' (Bivand et al., 2015) and 'raster' packages (Hijmans and van Etten, 2012) in R (R core
149 development team, 2016). One hundred random survey sites were selected within the shrimp
150 bed polygon in 2011. In 2012 the number of sites was increased to 150 and sampling locations
151 were selected using the pseudo-random Generalized Random-Tesselation Stratified (GRTS)
152 survey design (Kincaid and Olsen, 2015). Cross-validation tests of model accuracy showed that
153 population abundance estimates were not significantly improved by adding more survey points
154 so 100 survey points were again selected in 2014 (Tomczak, 1998).
155 Population surveys involved navigation to the pre-selected locations with a Trimble
156 GeoXT™ high precision GPS unit. At each site, burrow openings were counted within a 0.25 m^2
157 quadrat. After burrow counts were determined, 10 of the survey locations were randomly
158 selected to collect core samples. Core samples were taken randomly within the sampled
159 population to get a representative sample of the age structure and also determine the relationship
160 between shrimp density and burrow count for estimating total population abundance (Dumbauld
161 et al., 1996). Core sample locations were selected by dividing burrow quadrat locations into 5
162 different strata based on burrow density and randomly selecting 2 points within each of the 5
163 strata (Fig. 1). Core samples were taken with a 0.125 m^2 stainless steel core to 60 cm depth at
164 each randomly selected location. The number of shrimp burrows within the core area was
165 recorded prior to pushing the core into the substrate then material from each core was excavated,
166 sieved with 3mm mesh and sorted to collect shrimp. All shrimp were sexed and measured for
167 carapace length (CL) prior to being frozen at -80°C for lipofuscin age analysis. A minimum
168 sample size of 200 animals is preferred for accurate age structure analysis (Kritzer et al., 2001).
169 If a total of 200 individuals were not collected in the first 10 core samples, randomly selected

170 "back-up" core locations were sampled in the high-density strata until the minimum sample size
171 was reached. Sex ratios were examined for equal proportions using a chi-square proportions test.
172

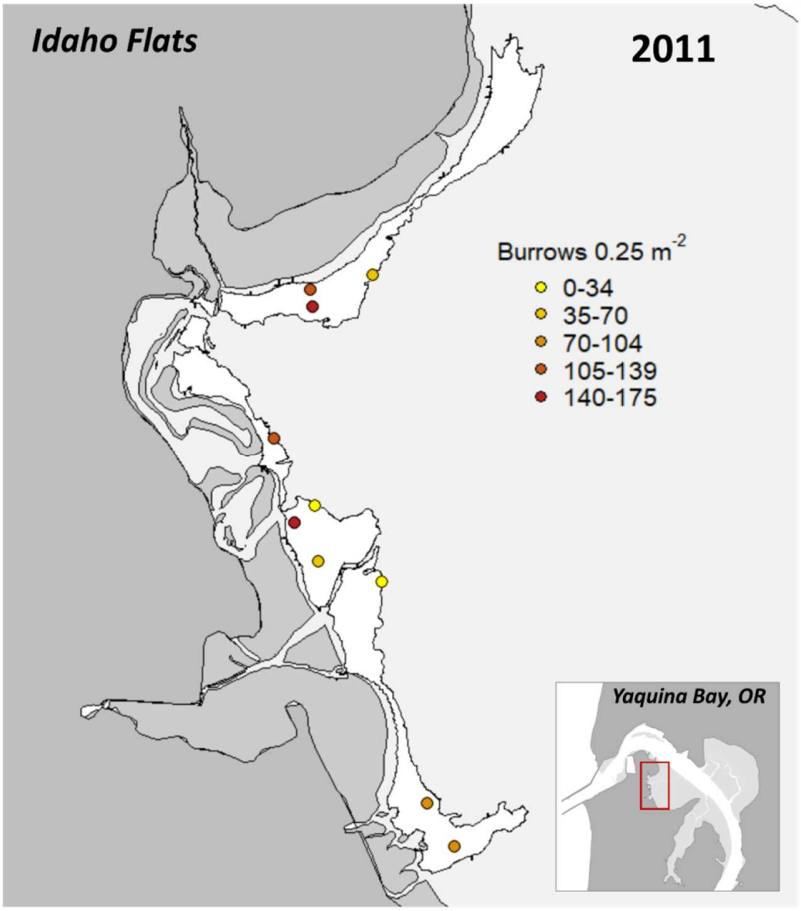

173

174 **Figure 1.** Shrimp population polygon (white) from 2011 sampling period with survey locations
175 overlaid. Crosses indicate quadrat sample sites and colored circles showing stratified core
176 sampling sites. Darker grey regions represent land/marsh, lighter grey is intertidal flats. The inset
177 shows a map of Idaho Flats region in Yaquina Bay, Oregon, USA (44°37'8.4"N, 124° 2'27.2"W)
178 where *Neotrypaea californiensis* were sampled from 2011-2104.

179 **2.3 Spatial interpolation model for shrimp abundance**

180 Estimation of total shrimp number relied on the relationship between the number of
181 burrows and the number shrimp. This relationship was determined by conducting simple linear
182 regression of shrimp number (m^{-2}) as a function of burrow number (m^{-2}) for each year of the
183 survey. Separate models were generated for each year because ANCOVA which included year as
184 a covariate indicated a significant interannual variation in the relationship (year effect; $F = 3.51$,
185 $p = 0.025$). The regression model for each year was then used to convert burrow counts to shrimp
186 numbers for estimation of total population abundance with a deterministic spatial interpolation
187 model.

188 An inverse distance weighted (IDW) spatial interpolation model was used to estimate
189 total shrimp abundance within the area sampled using the 'raster' package in R (Hijmans and van
190 Etten, 2012). Ideal parameters for the IDW model were determined with cross-validation of IDW
191 models (Tomczak, 1998) using combinations of inverse distance weighted power (idp) values
192 ranging from 0.5 to 3 and number of neighbors (nmax) from 2 to 18. The models were most
193 accurate with idp = 1.5 and nmax = 6; these values were used for estimating shrimp abundance
194 for all years using a 5 m^2 cell size. The interpolation model was bounded by the shrimp bed edge
195 polygon and total abundance was estimated as the sum of shrimp abundance over all cells within
196 the polygon. Variance for total abundance estimates was determined using the blocked
197 bootstrapping method with the 'sperrorest' package (Brenning, 2012) and accounted for the
198 spatial autocorrelation of the survey data (Lahiri et al., 1999; Lahiri and Zhu, 2006).

199

200 **2.4 Estimation of lipofuscin-based population age structure**

Age structure was estimated with cohort analysis of lipofuscin frequency histograms. Lipofuscin levels were determined for all shrimp greater than 6.0 mm carapace length collected in population surveys using methods described in Bosley (2016). Shrimp brain tissue was dissected, placed in a pre-combusted 1.5 ml amber vial and topped with 1.0 ml dichloromethane:methanol (2:1) solution. Samples were sonicated for 30 seconds at 18% with a microprobe sonicator then stored in the freezer overnight to ensure complete extraction of lipofuscin. Samples were then dried completely with pure N_2 and reconstituted with 0.25 ml HPLC-grade methanol. Lipofuscin was measured with an Agilent 1100 scanning fluorescence detector at excitation wavelength 281 nm and emission wavelength 615 nm using methanol as a carrier solvent. Fluorescence peaks were maximized with a sample volume of 15 µl and a flow rate of 0.8ml min^{-1}. Lipofuscin concentration was quantified by calibrating fluorescence values to a standard of quinine sulfate in 0.1 N H_2SO_4. Following lipofuscin measurement, samples were prepared for protein analysis by evaporating samples to dryness with pure N_2 and reconstituting with 1 ml of 16% deoxycholic acid. Samples were sonicated in an ice-water bath sonicator for 30 min and stored in a refrigerator overnight before protein quantification. Protein concentration was measured with an Agilent 1100 fluorescence detector at excitation 280nm and emission 345 nm using nanopure water as a carrier solvent. Peaks were maximized with a 12 µl sample volume and 0.8 ml min^{-1} flow rate. Fluorescence intensity of extracted protein was calibrated with a standard of bovine serum albumin (BSA) in 16% deoxycholic acid (Harvey et al., 2010; McGaffin et al., 2011). The lipofuscin metric used in the analysis was a relative concentration index where the total concentration of lipofuscin in the tissue extract is normalized to the total protein with units: ng lipofuscin μg^{-1} protein. The normalized index, LF Index, is used to account for variation in animal size and tissue dissection efficiency.

Males and females were combined to ensure a sufficient number of specimens for the cohort analysis and because lipofuscin accumulation rate is not significantly different between the sexes (Bosley, 2016). The cohort analysis was conducted by dividing lipofuscin frequency distributions into a mixture of Gaussian probability curves, each representing an estimated age class. The analysis was completed separately with data from each year using the package 'mixdist' (MacDonald and Du, 2012) in R. The 'mixdist' algorithm works by applying maximum likelihood methods to estimate means and variance for a mixture of distributions based on preselected starting values and application of constraints on the parameters (Du, 2002). An LF Index bin size of 0.20 ng ug^{-1} was used for the analysis because it allowed for the greatest resolution of potential modes the histogram. Initial starting values were selected visually based on where modes appeared to be present. No additional constraints were placed on parameter values and the model for each year was tested for goodness-of-fit using a chi-square statistic. Ages were assigned to modes present in frequency histograms based on mean and standard deviation for the lipofuscin accumulation rate from previous growth experiments conducted on *N. californiensis* (Bosley, 2016; Bosley, unpublished, 1.43 ± 0.06 ng μg^{-1} yr^{-1}).

2.5 Estimation of shrimp mortality rate

The average annual mortality rate for *N. californiensis* in Yaquina Bay was determined using a catch-curve analysis (Robson and Chapman, 1961) of numbers-at-age for cohorts with ages collected over the four-year survey. We were not able to age juvenile shrimp (shrimp < 6.0 mm, < 2-year-old) because these shrimp were too small for precise protein quantification and therefore they do not appear as part of the lipofuscin-based age structure. The total abundance of adults in each year was determined by subtracting the proportion of juveniles from total

abundance estimates. Adult shrimp abundance was converted to numbers-at-age based on the proportion-at-age determined from the lipofuscin-based cohort mixture analysis described above. Variances for the abundance estimates were determined using the standard formula for calculating the product of two variances. Age frequency histograms indicated that our survey methods did not fully select shrimp less than age 4 in core samples. It is not possible to accurately determine lipofuscin concentration in shrimp <6.0 mm in body length, primarily due to the small brain size and very low concentration of brain tissue protein. In addition, variable growth rates and patchy distributions of young shrimp can affect quantification of sub-adult *N. californiensis* (Dumbauld and Bosley, 2018). By age 4, we assumed that all animals had grown to a size where they captured with our sampling methods and had achieved a size where LF analysis could be done, thus our mortality model only included numbers-at-age data for shrimp age 4 and older.

Mortality was estimated by determining the rate of decline in shrimp number as each cohort progressed through time by fitting a discrete-time exponential decay mortality function to the numbers-at-age data for all cohorts aged 4 and greater combined:

$$N_{c,a+1} = N_{c,a} e^{-k_c} \quad (1)$$

Where $N_{c,a}$ is the number of individuals in a cohort c at age a, $N_{c,a+1}$ is the number of animals in a cohort c alive at age $a+1$ and k_c is the cohort-specific exponential decay coefficient (instantaneous mortality rate).

Annual mortality rate (M) was determined using the linearized form of the model which allowed k to be estimated as the slope of the regression

$$log(N_{a+1}) = -k + log(N_a) \quad (2)$$

Annual survival fraction (*S*) was estimated by back-transforming the slope (with bias correction; Newman 1993):

$$\bar{S} = e^{-\bar{k}+0.5\sigma_k^2} \quad (3)$$

where σ_k^2 is the estimated variance of k. Annual mortality (*M*) for each cohort was then estimated as:

$$\bar{M} = 1 - \bar{S} \quad (4)$$

The difference in mortality rate across cohorts was tested with ANCOVA which included cohort as a covariate. A sum-of-squares F-test was used to compare full models which included cohort (additive and interactive effects) to a reduced model that included only age as a predictor variable. Average mortality rate and the associated error estimated from the best model was then used to conduct population simulations.

2.6 Life-Table Population Simulations

A perturbation analysis was done to test the effects of changes in mortality and recruitment on the population dynamics of *N. californiensis*. This theoretical analysis explored the response of population density under different recruitment and mortality scenarios. The model assumed recruitment into the adult population occurred at age 2 years, the age at which the shrimp are initially captured in our survey as determined from lipofuscin-based age structure, and lifespan for *N. californiensis* was 13 (A_{max}) based on previous estimates for the longevity of the species (Bosley and Dumbauld, 2011) and therefore shrimp were assumed to exit the model after age 13. For the simulations, it was assumed that the mortality rate was constant across all age classes in the model.

294

295 **2.6.1 Single cohort mortality calculations**

296 The effect of mortality rate on the population density of a cohort was investigated by
297 evaluating the cohort model equations over a range of mortality levels (Equation 5). The
298 mortality rates that we tested were 0.9, 0.5, 0.3, and 0.1 yr^{-1}.

299

300 $$N_a = N_2(1 - M)^{a-2} \quad (5)$$

301

302 **2.6.2 Multi-cohort equilibrium scenarios**

303 Projections of the cohort model were completed to examine the outcome of different
304 combined recruitment and mortality scenarios. Population density was modeled assuming
305 constant annual recruitment and constant mortality in the following four scenarios: high
306 recruitment / low mortality; high recruitment / high mortality; low recruitment / high mortality;
307 low recruitment / low mortality. High and low mortality rates were assumed to be 0.8 and 0.2 yr^{-2},
308 respectively. High and low recruitment values were modeled as 60 and 20 shrimp m^{-2},
309 respectively. These recruitment values were selected because they represent the range of
310 recruitment values that may be expected based on empirical settlement data from Yaquina Bay,
311 Oregon (Dumbauld and Bosley, 2018). The multi-cohort equilibrium scenario modeled
312 population dynamics using the following equations:

313 $$N_{2,t} = R_t \quad (6)$$

314 $$N_{a+1,t+1} = N_{a,t}(1 - M) \quad (7)$$

315

316 **2.6.3 Stochastic Recruitment Model**

A stochastic model was constructed that allowed recruitment rate to vary annually. This was done by setting recruitment (entry of age 2 shrimp into the model) as a random variable with a negative binomial distribution (mean = 11 and dispersion = 0.4). These parameters were estimated by fitting a negative binomial distribution to age 2 density data from surveys conducted in Yaquina Bay from 2005 – 2015 (Dumbauld and Bosley, 2018). This model assumed that mortality rate was constant within a cohort but was allowed to vary across cohorts by setting k as a normal random variable with a mean and standard deviation equal to the mortality fraction determined from ANCOVA (described above). Projections were done into a t_{max} x A_{max} matrix where t_{max} = the total number of time steps in the model. Numbers-at-age for each cohort was calculated with the following equation:

$$N_{a+1,t+1} = N_{a,t}e^{-X} \quad (7)$$

Where,

$$X \sim Normal(k, \sigma_k) \quad (8)$$

Total shrimp numbers were converted to shrimp density (m^{-2}) by summing numbers-at-age for each time step and dividing by total area (A).

$$ShrimpDensity_t = \frac{1}{A}\sum_{a=1}^{n} N_{a,t} \quad (9)$$

The mean and variance for shrimp density at each time step was determined for the stochastic scenario with a Monte Carlo simulation procedure where calculations were repeated 500 times. Each model was projected for 15 years, a suitable amount of time to enact a management plan.

340

341 **3. RESULTS**

342 **3.1 Population Demographics**

343 The total area occupied by *N. californiensis* changed over the four years that our surveys
344 were conducted showing a peak in 2013 with the population covering 91,596 m^{-2} (Table 1, Fig.
345 2). The total number of shrimp in the area sampled ranged from a high of 7.1 million in 2013 to
346 3.9 million in 2014. Shrimp abundance increased by 34.1% from 2012 to 2013 and decreased by
347 14.3 % and 44.3% from 2011 to 2012 and 2013 to 2014 respectively. Despite the fluctuations in
348 total shrimp numbers, overall shrimp density declined over the four years (~50%) surveyed. The
349 decline in density was evident in spatially interpolated maps of the surveyed shrimp population
350 which also showed expansion of the shrimp bed to the north in 2013 and in 2014 a large extent
351 of the population to the south had disappeared (Fig. 2). The burrow opening-to-shrimp
352 relationship also varied slightly each year with the steepest slope in 2011; ~2 burrows for every
353 shrimp (Table 2). In 2013 and 2014 the ratio declined to ~3 burrows per shrimp (Table 2, Fig. 3).

354

355

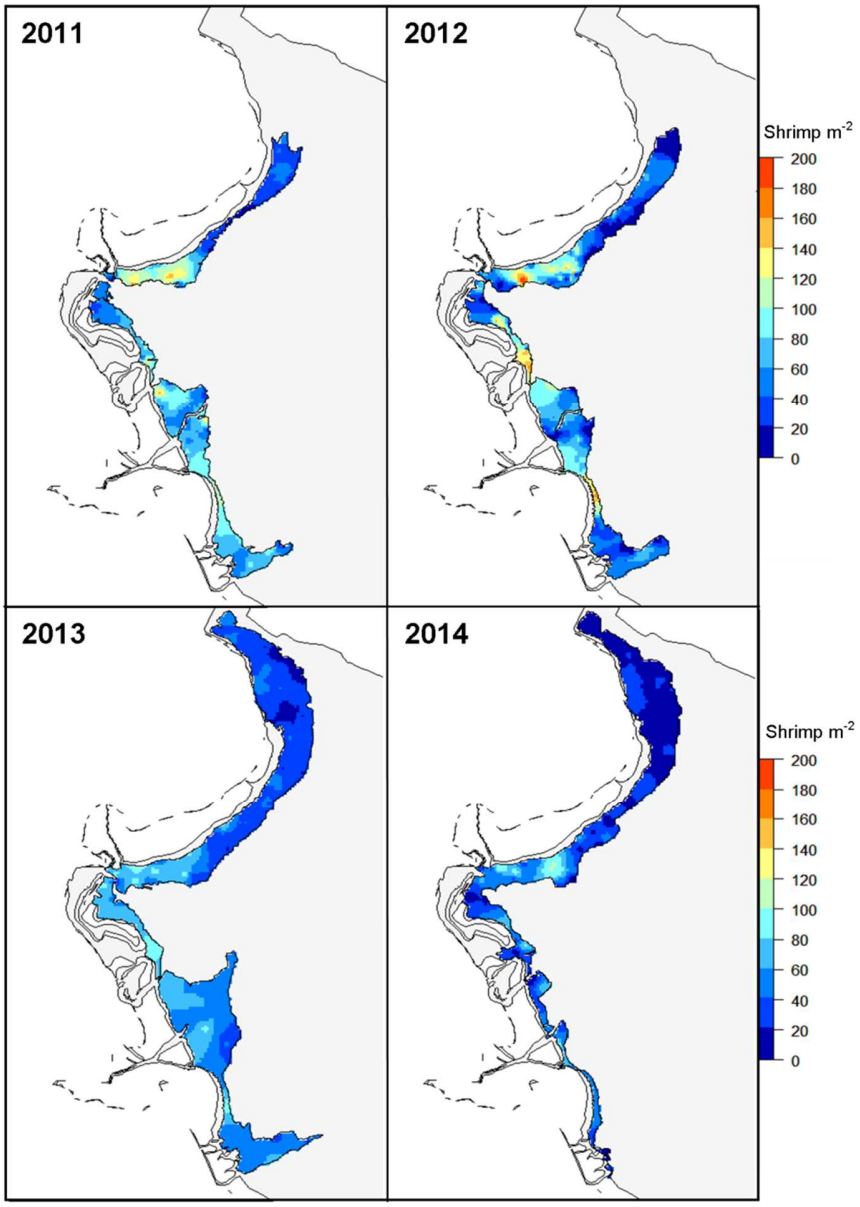

Figure 2. Inverse distance weighted interpolation maps of *N. californiensis* population density determined from annual sampling of the Idaho Flats region in Yaquina Bay, Oregon (2011 – 2014). Warm colors indicate high shrimp densities. The white area represents land and light grey represents intertidal flats.

362

363

364

365

Year	N	Area (1000 m^2)	Population Size (10^6)	SD (10^6)	% Change	Mean Density (shrimp m^{-2})
2011	105	44.92	6.178	0.211	na	137.54
2012	154	56.26	5.293	0.237	-14.33	94.07
2013	145	91.60	7.098	0.242	+34.09	77.49
2014	100	58.07	3.955	0.830	-44.28	68.10

366

367 **Table 1.** Table showing population statistics from data collected during annual surveys of *N.*
368 *californiensis* in Yaquina Bay, Oregon. Estimated population size from each survey year is based
369 on Inverse Distance Weighted (IDW) interpolations. N; sample size, SD; standard deviation.

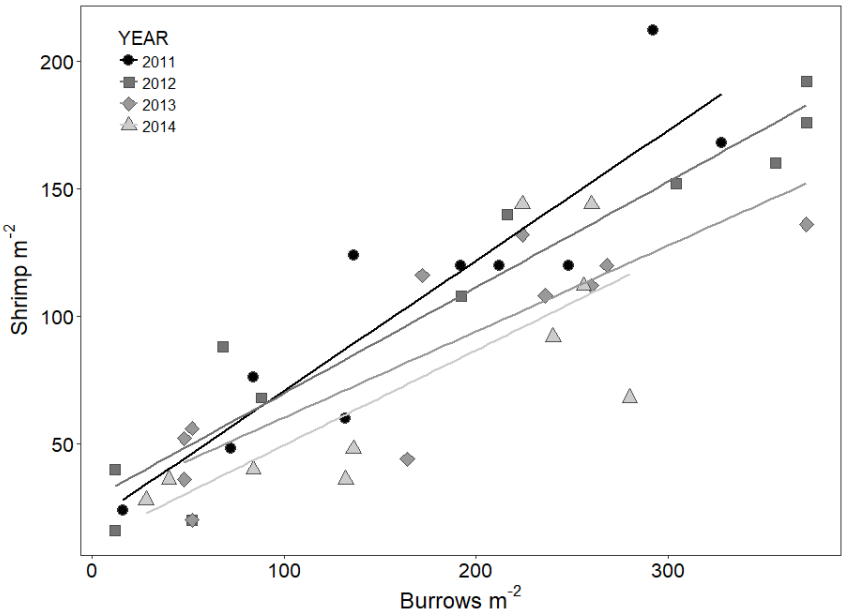

Figure 3. Linear regression analysis of burrow number to shrimp number used to estimate shrimp abundances from burrow counts in each survey year. Regression coefficients are presented in Table 2.

Coefficient	2011	2012	2013	2014	Pooled
Intercept	19.75 (16.55)*	28.38 (9.34)*	26.56 (12.80)*	12.26 (19.69)	21.63 (7.57) *
Burrows m^{-2}	0.51 (0.08)*	0.42 (0.04)*	0.34 (0.06)*	0.37 (0.10)*	0.41 (0.04)*
d.f.	8	9	9	8	40
adj r^2	0.8	0.914	0.733	0.572	0.752

Table 2. Coefficients with standard errors from the regression analysis of burrow opening number to shrimp number relationship from four years of surveys conducted on Idaho Flats in Yaquina Bay. (*) indicates statistically significant ($p<0.05$), d.f.; degrees of freedom.

401 Carapace lengths of shrimp sampled in cores indicated a fairly stable size structure.
402 Juveniles were clearly evident in core samples from 2011 and 2012, presumably shrimp that had
403 recruited to the population as post-larvae the previous year (Fig. S1). Juveniles (shrimp < 6.0 mm
404 CL) made up 17.3% and 12.3% of the total population in 2011 and 2012 respectively. There
405 were few small shrimp collected in 2013 and 2014 core samples (Table S1). Average adult CL
406 was similar across years averaging around 10 mm in 2011, 2012, and 2013 but was slightly
407 smaller on average in 2014 (mean CL = 9.78 ± 1.65; Fig. S1). The sex ratio of adults appeared to
408 be dominated by females (~2:1) in all years but the difference was only statistically significant in
409 2011 ($X^2 = 8.741$, p = 0.003; Table S2).
410 The mixture of Gaussian distributions determined with the 'mixdist' model fit the actual
411 LF Index frequency data as determined by chi-square goodness-of-fit tests (Table S3), but there
412 was a fair amount of overlap between the different curves. Evaluation of population age structure
413 showed age structure to be stable over the four years with ages 2 to age 7 present in core samples
414 with the exception of 2014 when 6-year-old shrimp were absent in the core samples. In all years,
415 age 4 animals were the dominant year class in our samples (Table S3). This was likely a result of
416 variable growth rates causing only a fraction of age 2 and 3 animals being large enough for LF
417 analysis (<6.0 mm CL). By age 4, all animals had likely grown to a size where they were
418 captured with our sampling methods and where age analysis could be done (Figs. 5 & S1).
419
420
421
422
423

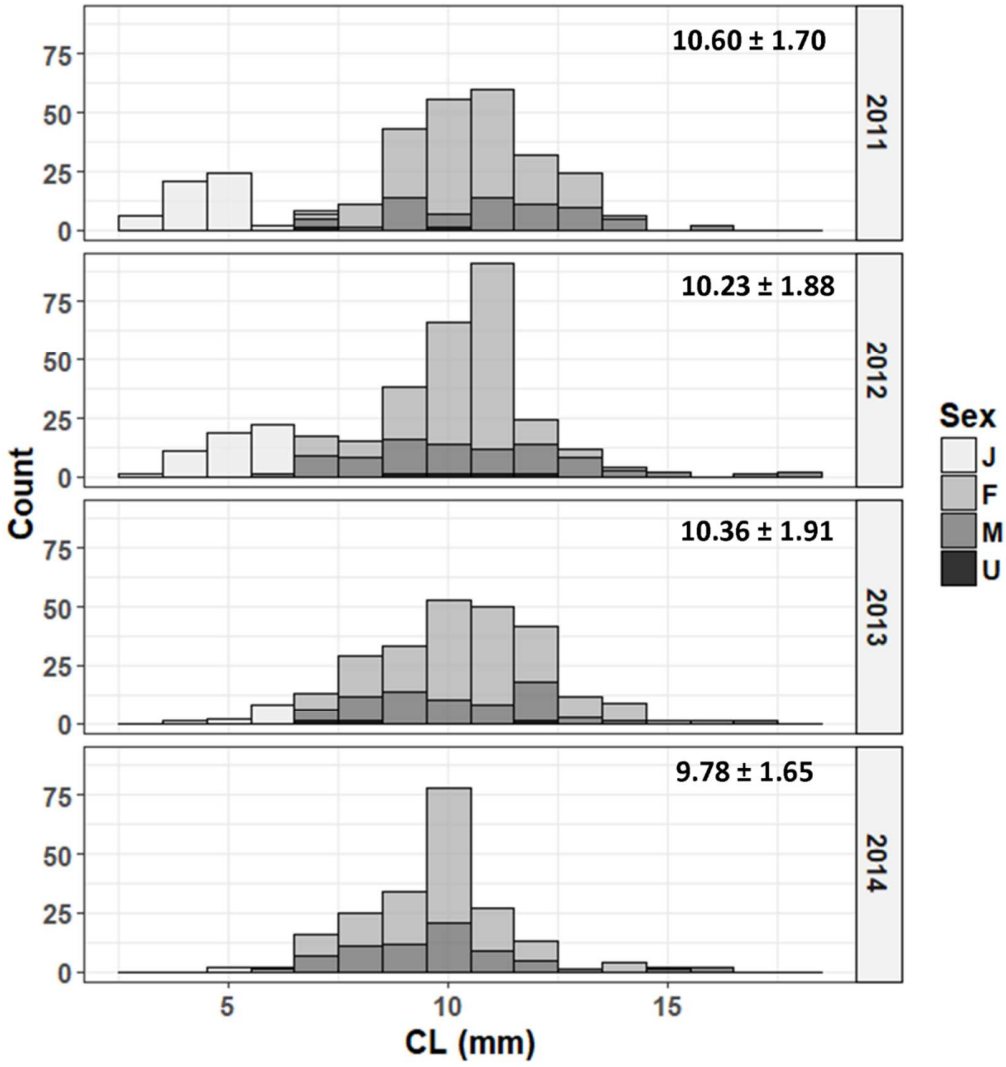

Figure 4. Carapace length frequency distributions of *N. californiensis* collected from annual population surveys on Idaho Flats. Bars are divided by maturity and sex. Mean carapace length (mm) and standard deviation for each year is shown in the upper right corner of each panel. Juveniles are animals < 6.0 mm CL and were not aged using lipofuscin. J; juvenile, F; female, M; male, U; adult of unknown sex.

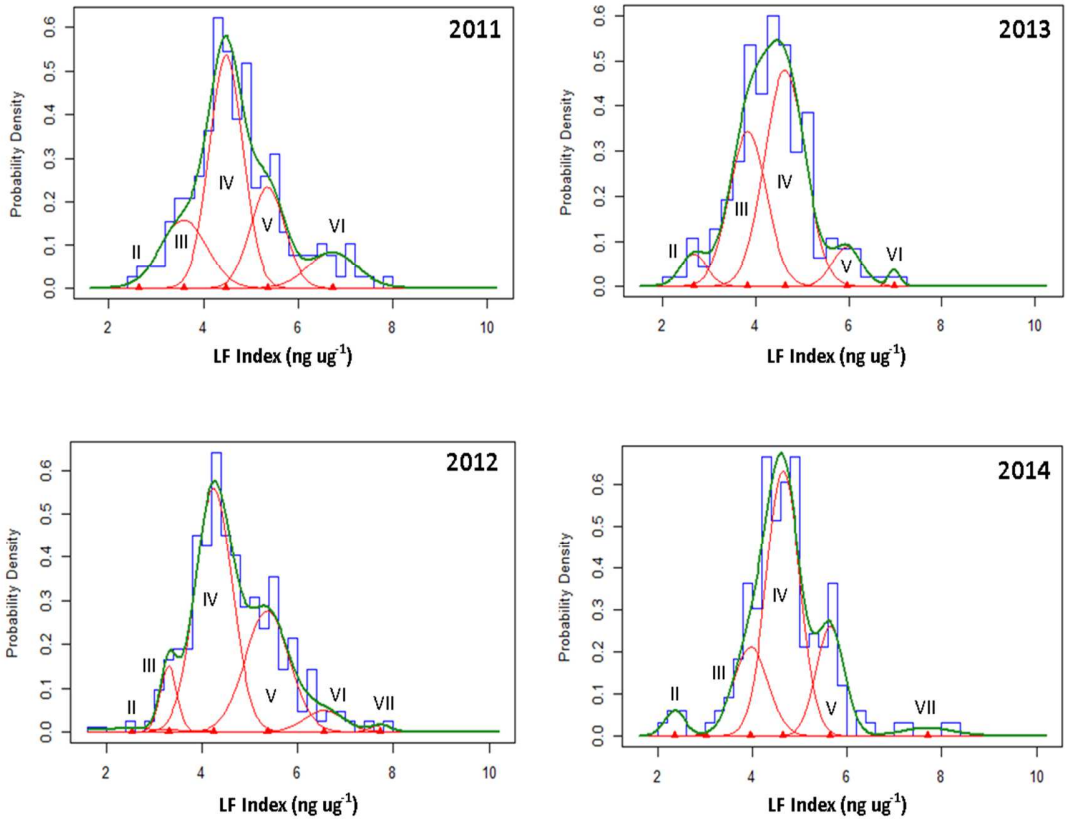

Figure 5. Results for model progression analysis of lipofuscin frequency data from annual surveys using the 'mixdist' package in R (McDonald and Du, 2012). Age class assignments and proportions are shown in Table 3. Red lines denote best fitting mixture components with means denoted as triangles along the x-axis. The green line denotes full model fit to LF Index frequency distribution. Age classes are shown with Roman numerals and were selected based on the mean LF accumulation rates recorded for *N. californiensis* (Bosley 2016; Bosley, unpublished, 1.43 ng μg^{-1} yr^{-1}).

442

443

	Age Only	Age + Cohort	Age * Cohort
Coefficient	Estimate (SE)	Estimate (SE)	Estimate (SE)
Intercept	19.981 (0.781)*	21.2842 (1.723)*	29.732(8.514)
Age (yrs)	-1.281 (0.146)*	-1.451 (0.255)*	-2.751 (1.306)
CohortB	-	-0.168 (0.720)	-8.070 (11.159)
CohortC	-	-0.405 (0.636)	-9.787 (8.824)
CohortD	-	-0.844 (0.845)	-8.404 (10.366)
CohortE	-	-0.429 (0.844)	-8.409 (10.366)
CohortF	-	-0.890 (1.042)	-4.138 (3.455)
Age*CohortB		-	1.201 (1.847)
Age*CohortC		-	1.470 (1.370)
Age*CohortD		-	1.102 (1.847)
Age*CohortE		-	1.196 (1.847)
Age*CohortF		-	NA
N	13	13	13
adj R^2	0.863	0.797	0.619
	F	0.152	0.217
	p	0.96	0.968

444

445 **Table 3.** Coefficients from linear models of log-transformed numbers-at-age used to estimate
446 mortality rate. The sum of squares F-test was used compare the full models containing cohort
447 and age with a reduced model containing age only.

448

449

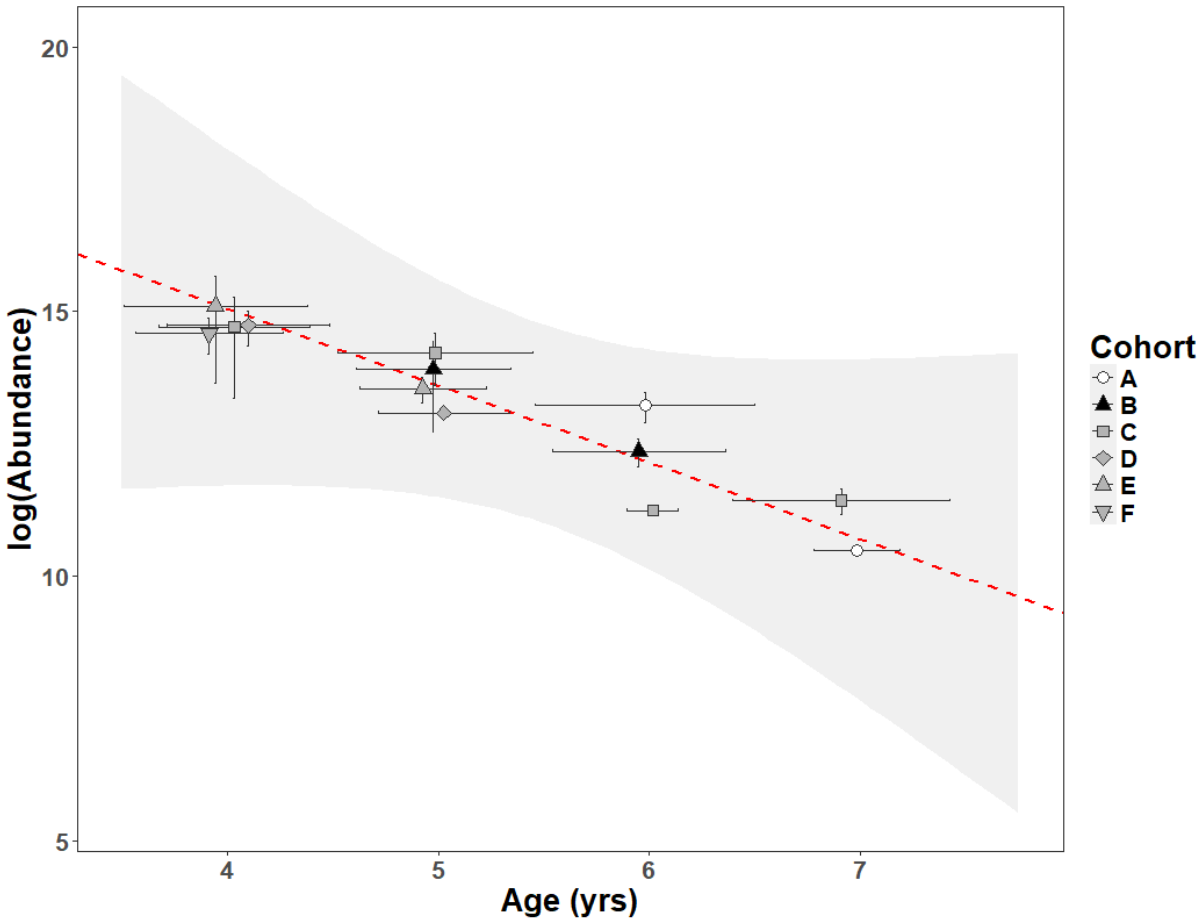

450

451 **Figure 6.** ANCOVA results used to estimate mortality rate using Eq. 2. Mortality rate was not
452 found to be statistically different among cohorts. Different point types represent numbers-at-age
453 for separate cohorts as they progress through time. Error bars show standard error for estimates
454 of lipofuscin-based age (x-axis) and for shrimp abundance-at-age (y-axis). The shaded area
455 represents 95% confidence interval for the estimate of mortality rate from full model (Table 4).
456 Points are jittered for visualization.

457 Mortality rate, estimated with Equations 2-4, was determined to be 0.757 yr^{-1} (95% CI;
458 0.613-0.858 yr^{-1}) after controlling for variation across cohorts. Comparison of the full models
459 which contained cohort as covariate vs. the reduced model indicated that cohort was not a
460 significant predictor of mortality rate for *N. californiensis* on Idaho Flats (Fig. 6, Table 3).
461 Mortality rate estimated from the reduced model was 0.719 yr^{-1} (95% CI; 0.633-0.793 yr^{-1}).
462

463 **3.2 Life-Table Population Simulations**

464 Theoretical life-table projections showed that a single cohort experiencing the mortality
465 rate of 0.719 yr^{-1} would be reduced to very low population densities after 4 years (0.6% of
466 original abundance) regardless of recruitment strength (Fig. 7a). Conversely, changes in
467 mortality rate had a pronounced effect on the density of a cohort over time (Fig. 7a). The
468 combined scenarios assumed that annual recruitment and mortality rates were constant which
469 allowed prediction of change in population density as the population reached equilibrium with
470 multiple overlapping generations (Fig. 7b). The low mortality and high recruitment scenario
471 showed that following colonization a population can achieve a high density approaching
472 equilibrium in 20 years (Table S4). The low recruitment example showed population densities
473 increasing slowly to a much lower equilibrium density (Fig 7b). In both high mortality scenarios,
474 the population reached equilibrium quickly (4 years) and was maintained at overall low densities
475 (Fig 7b, Table S4).
476
477
478

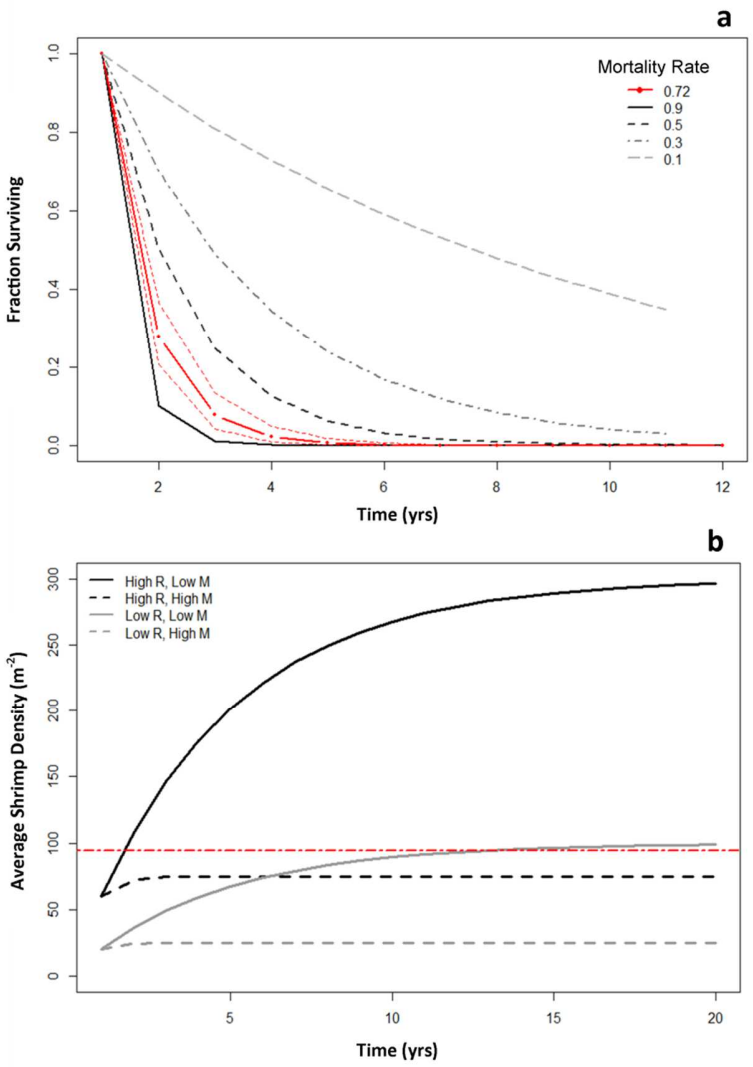

479

480 **Figure 7.** Prediction for changes in population density calculated in life table scenarios. a) The
481 single cohort example under different mortality scenarios. Red line indicates measured mortality
482 for *N. californiensis* with the dashed line representing 95% confidence interval. b) Multi-cohort
483 example with population projected to equilibrium under different combinations of constant
484 recruitment and mortality. Mortality was modeled at 0.2 yr^{-1} and 0.8 yr^{-1} for low and high
485 scenrios, respectively. Recruitment (at age 2 years) was modeled at 20 and 60 shrimp m^{-2}. Red
486 line represents the actual average density for *N. californiensis* determined over the 4-year survey
487 (94 shrimp m^{-2}).

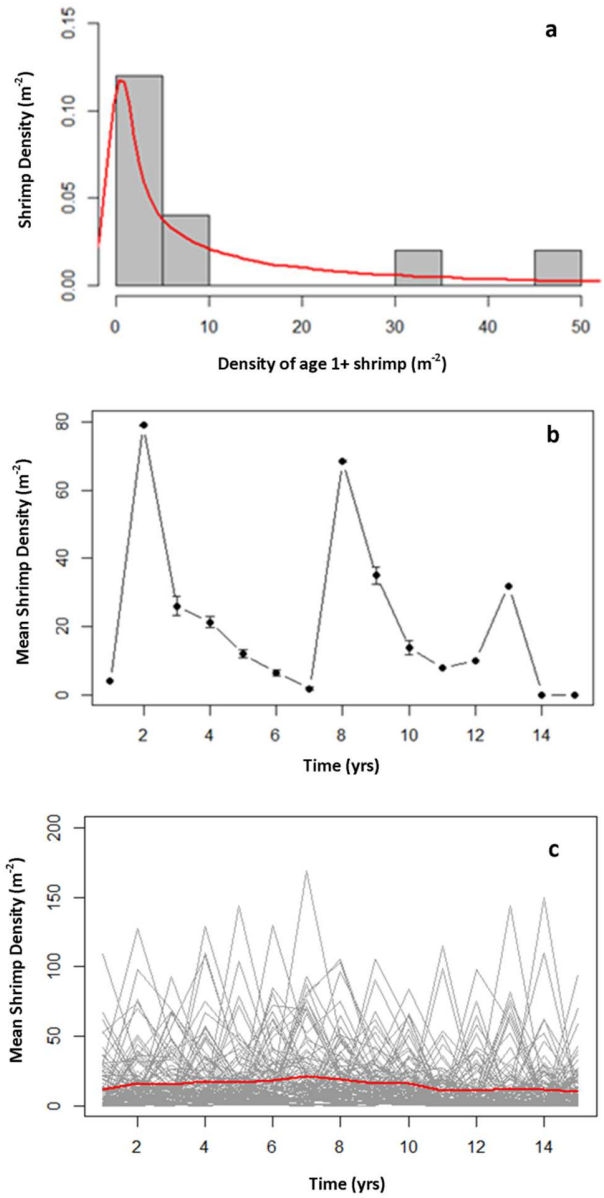

488

489 **Figure 8.** a) Negative binomial probability distribution for estimating numbers of 2-year-old
490 shrimp in monitoring surveys of *Neotrypaea californiensis* in Yaquina Bay from 2005 – 2015
491 from Dumbauld and Bosley (2018). The bar plot shows real data and density curve represents the
492 probability distribution function (mean = 11 and dispersion = 0.4). b) Predictions of population
493 density from a single iteration of the stochastic recruitment scenario c) Results of 500 iterations
494 of the stochastic recruitment model used to estimate the average long-term population density
495 (14.98 shrimp m^{-2}).

The stochastic model assumed recruitment of age 2 shrimp occurred at low levels with periodic large events (Figs. 8a & 8b), which is reflective of actual measurements from population surveys in Yaquina Bay. As the cohorts progressed through the model, population density tended to decrease until the next major recruitment event occurred. The average density estimated from 500 iterations of the stochastic model was 14.98 shrimp m^{-2} (Fig. 8c) which suggests that a small population can persist with generally low and infrequent recruitment.

4. DISCUSSION

The ability to accurately age crustaceans has hindered the application of standard age-structured models for estimating vital rates for these invertebrates (Hartnoll, 2001; Bosley and Dumbauld, 2011; Punt et al., 2014). Recent developments of alternative aging techniques (O'Donovan and Tully, 1996; Ju et al., 2003; Puckett et al., 2008; Harvey et al., 2010) and improved methods of population assessment have created the opportunity to understand crustacean population dynamics in a way that was not previously possible. The primary goal of this study was to apply contemporary methods to estimate the average annual mortality rate for a population of *N. californiensis* in Yaquina Bay, Oregon, and determine if that rate was constant over time. The cohort-based approach showed an exponential decay function described burrowing shrimp mortality rate at a single sampling location and this function was not statistically different among cohorts. In addition, the mortality rate we estimated from lipofuscin-based measurements of age was consistent with similar estimates of mortality determined from size class analysis of *N. californiensis* and other thalassinidean shrimps. Feldman et al (2000) tracked cohorts of *N. californiensis* over two years and estimated mortality rates to be 0.75 yr^{-1} and 0.22 yr^{-1} for males and females, respectively, but the authors had difficulty in estimating the

519 parameter when females immigrated from outside the sample area. Conides et al. (2012) found
520 natural mortality rate of the mud prawn, *Upogebia pusilla*, to be 0.93 yr^{-1} and Pezzuto (1998)
521 calculated annual mortality rates of 0.78 yr^{-1} and 0.71 yr^{-1} for male and female *Neocallichirus*
522 *mirim*.
523
524 **4.1 Accuracy in estimating population parameters with lipofuscin**
525 The estimation errors associated with proportion and mean LF Index-at-age parameters
526 acquired from the 'mixdist' algorithm were quite large in some years. Even though the overall
527 model for a mixture of frequency distributions fit well, the high level of uncertainty in the
528 parameter estimates suggests that they are not highly robust. The modal progression analysis we
529 conducted uses a normal approximation to describe the distribution of lipofuscin concentration
530 within a cohort. While application of the Gaussian distribution is most common for conducting
531 age-structure analysis, lipofuscin concentration frequency data may be best described by a
532 different probability distribution, such as a Gamma distribution, and further work should be done
533 to refine cohort analysis as it applies to lipofuscin data. Uncertainty in the parameter estimates
534 may have resulted from fitting the model with limited constraints on the estimates, but could also
535 be explained by significant overlap of lipofuscin concentration distributions among cohorts.
536 The primary advantage of using analysis of lipofuscin to estimate crustacean age is that
537 accumulation rate may be consistent over broad temporal and spatial ranges and can provide an
538 index of age, despite clear differences in growth. *N. californiensis* has been previously shown to
539 have variable growth rates and in some cases, shrimp can molt to a smaller size when
540 environmental conditions are poor which has led to a decoupling of the age-size relationship both
541 within and across populations (Bosley and Dumbauld, 2011; Bosley, 2016). Even though growth

rates are variable, lipofuscin accumulation is fairly consistent across populations and across cohorts. Bosley et al. (2018) estimated lipofuscin accumulation rate in multiple cohorts grown in outdoor mesocosms and found 91% of the variability in LF Index value was explained by age, whereas body size was not correlated with chronological age. Our data showed significant overlap in LF index frequency histograms for each survey year. Because formation of lipofuscin is controlled by metabolic processes, the rate in which it accumulates is subject to considerable individual variability and has been linked to environmental conditions (i.e., temperature) under natural field conditions (Sheehy et al., 1995; O'Donovan and Tully, 1996). Laboratory and field experiments showed that temperature had only a weak effect on lipofuscin accumulation in *N. californiensis* (Bosley, 2016) but other factors that influence metabolic rates such as genetic background, oxidative stress, and salinity may be important in dictating lipofuscin accumulation (Terman, 2001; Allan et al., 2006; Hiebenthal et al., 2012).

The timing of recruitment may also explain, in part, overlapping modes in lipofuscin concentration frequency histograms. Settlement of *N. californiensis* typically occurs between July and October and but has been shown to occur as late as January or as early as March depending on the year and the location (Dumbauld et al., 1996; Dumbauld and Bosley, 2018). Extended long recruitment periods would increase variability in mean LF Index-at-age estimates, broadening modes and increasing overlap in frequency data. Despite these challenges in estimating "true" age for *N. californiensis* using lipofuscin concentration, the method has proven to be a more accurate metric of age than body size and allows for comparison across and within populations where growth rates can vary significantly.

Other issues in estimating mortality rates involve the assumptions of our simple cohort model. Two assumptions, in particular, have important effects on the validity of our estimates.

First is the assumption of a closed population, i.e. that there is no post-recruitment migration into or out of the sampling area, which is discussed in the next section. Second, we assume that mortality is constant across age or size and across cohorts. We did use an ANCOVA to test for cohort effects and found no significant differences, but the limited data implies that this test would have little power to detect any but extreme differences. At this time, we lack data to test for age or size effects, which would likely require tracking fates of individuals via tagging or other techniques.

4.2 Patchiness in shrimp distribution

Biological populations are primarily governed by two sets of opposing processes; recruitment and mortality; immigration and emigration. For sedentary or attached benthic species like *N. californiensis*, immigration and emigration are generally ignored because these animals exhibit little or no post-settlement movement (Rosenberg, 1974; Hewitt et al., 1997; Castorani et al., 2014). Therefore, observed patterns of abundance for benthic macrofauna are usually described by the opposing forces of recruitment and mortality (Olaffsson, 1994). Because of their limited motility, these processes likely act on populations at a fine scale, resulting in a mosaic of densities across the landscape (Thrush, 1991; Hewitt et al., 1997; Lundquist et al., 2010). The burrow count densities we encountered ranged from 0 to >200 burrows m^{-2} and exhibited clear spatial structure showing "hotspots" of high density in localized regions. Patchy distributions of benthic species have been studied for several decades with most work being focused on settlement and subsequent recruitment as the primary process controlling populations (Underwood and Fairweather, 1989; Morrisey et al., 1992; Fraschetti et al., 2002). Long-term settlement records for *N. californiensis* in Yaquina Bay have shown annual recruitment patterns

588 to be sporadic with relatively low shrimp numbers recorded each year on average, yet adult
589 populations persist in high densities in some areas (Dumbauld and Bosley, 2018). Population
590 projections of the cohort model in our study show that high population density can be explained
591 by either high survival rate, high recruitment or both.

592 To date, much of the population data collected on *N. californiensis* has been from areas
593 with dense shrimp populations (Bird, 1982; Dumbauld et al., 1996; Feldman et al., 2000; Bosley
594 and Dumbauld, 2011). Bosley and Dumbauld (2011) used lipofuscin-based aging methods to
595 estimate age structure of *N. californiensis* in a high-density patch and found 13 age classes
596 present in their samples. Our projections showed shrimp density to be sensitive to changes in
597 mortality. Using the mortality equations, a cohort experiencing a low mortality rate of 0.1 yr^{-1}
598 would have only been reduced to 34.7 % of its original size after 10 years compared to <0.001%
599 in a cohort of the same size under the high mortality scenario (M = 0.72 yr^{-1}). These conditions
600 would broaden the age structure with the inclusion of a higher proportion of older shrimp in the
601 population and increase the estimated survival rate based on age-structure data (Udevitz and
602 Ballachey, 1998; Carey et al., 2008; Udevitz and Gogan, 2012). The survey we conducted was
603 designed to capture as much variability in age distribution and mortality as possible throughout
604 the area that we sampled and identify spatial changes to the overall population that would not
605 have been observed if only a single location had been surveyed. We observed only 7 age classes
606 using the lipofuscin aging method but sampling took place over a larger spatial extent and
607 covered areas of low population density where mortality is likely to be much higher, especially
608 along bed edges where environmental stressors or greater exposure to predators may limit
609 populations (Bertness et al., 1985).

610 The role of post-larval dispersal in regulating population dynamics in soft-bottom
611 systems has drawn interest as a process responsible for the flux of animals in and out of patches
612 (Olaffsson, 1994; Valanko et al., 2010; Pacheco et al., 2013). Following settlement, juveniles or
613 adults can be triggered to actively disperse by abiotic or biotic cues (Lenihan and Micheli, 2001;
614 Commito et al., 2005; Kumagai, 2006). In population surveys of *N. californiensis*, new settlers
615 are typically sampled within the dense shrimp beds along with the established adult population
616 and are often found in low abundance. This pattern is consistent with other studies that have
617 shown dense aggregation of adults inhibits settlement and recruitment of juveniles through direct
618 feeding (i.e. cannibalism) or disruption of sediments (Bertness et al., 1985; Woodin, 1976;
619 Olaffsson, 1994). Our multi-year survey showed an expansion of the shrimp population that was
620 likely a result of a settlement event in 2010 (Dumbauld and Bosley 2018). However, densities in
621 the newly colonized area were initially low and declined following colonization. With a
622 mortality rate of 0.719 yr^{-1}, reduction in abundance was likely a result of natural mortality but it
623 may have also involved some migration of adults to replenish loss within a nearby high-density
624 patch. Some horizontal movement of adult *N. californiensis* has been documented (Peterson,
625 1984; Posey, 1986; Castorani et al., 2014) and there are numerous anecdotal reports by oyster
626 growers and bait harvesters that shrimp move in the water column (Dumbauld, 1994). Low-
627 density areas or bed edges may provide refugia for juveniles to settle and grow before recruiting
628 to the adult population. This "edge effect" was observed for *N. californiensis* in Yaquina Bay
629 (Dumbauld and Bosley 2018) and has been observed in other benthic invertebrates suggesting it
630 could be an important process in population regulation (Tamaki and Ingole, 1993; Whitlatch et
631 al., 1998; Minchinton, 1997). Further investigation into the movement of adult and sub-adult
632 shrimp within shrimp aggregations would confirm whether immigration is a factor to consider in

633 describing the population dynamics of *N. californiensis.* In addition, a greater understanding of
634 the settlement process and the primary causes of mortality following settlement would provide
635 insight into how shrimp populations persist in a heterogeneous estuarine environment.
636
637 **4.3 Predicting population change with a cohort-based model**
638 Like many benthic species with prolonged larval periods, *N. californiensis* populations
639 are "open" in that larvae are flushed from estuaries into the nearshore coastal ocean and therefore
640 recruits can come from distant populations (Fairweather, 1988; Underwood and Fairweather,
641 1989; Grosberg and Levitan, 1992; Caley et al., 1996) and some researchers have been
642 successful in linking recruitment strength of marine invertebrates to climate variables (Caley et
643 al., 1996; Shanks and Roegner, 2007; Menge et al., 2009; Menge et al., 2011; Woodson et al.,
644 2012). No studies to date have been able to do the same for predicting settlement in *N.*
645 *californiensis.* We constructed a cohort model which allowed for a theoretical investigation of
646 population-level changes resulting from different recruitment and mortality scenarios.
647 Recruitment in our model was defined as animals that enter a population at age 2, when they
648 have attained a size in which all sampled animals of that age (and older) are likely to be retained
649 on a 3mm mesh sieve. The model makes no assumptions about how the animals arrived, whether
650 through immigration or settlement, but also assumed that the shrimp will not migrate out of the
651 population following recruitment. In addition, we assumed that projected changes in cohort
652 density are a result of mortality only. While these assumptions may be simplistic, the application
653 of a simple model with minimal data requirements can provide a useful tool in the development
654 of management frameworks.

As the oyster industry in the Pacific Northwest has moved towards an integrated pest management strategy for these shrimp, the need to understand how populations change on oyster grounds following a settlement event has been a primary focus of ecological research on *N. californiensis* (Dumbauld et al., 2006; Dumbauld and Bosley, 2018). Based on empirical estimates of mortality, our model showed that a cohort can experience rapid decay in abundance following a colonization event. This result suggests that a population may be reduced to levels below which they can have a significant negative impact on oysters a few years following settlement (Feldman et al., 2000), even after a relatively high recruitment event. The single cohort example is somewhat unrealistic, however, because large settlement events for *N. californiensis* occur consecutively and/or periodically (Dumbauld et al., 2006; Dumbauld and Bosley, 2018). In species with multiple overlapping generations, regular settlement causes populations to increase in size as the year classes are effectively stored in the population (Cole, 1954; Chesson, 1983; Caswell, 2001). This observed pattern in *N. californiensis* (Dumbauld et al., 1996; Feldman et al., 2000; Bosley and Dumbauld, 2011) results in a stable size and age distribution which has also been observed for other similar burrowing shrimp species (e.g. *Nihonotrypaea harmandi,* Tamaki et al., 1997). Consequently, prolonged periods of repeated recruitment like those observed in the early 1990's in Willapa Bay (Dumbauld and Bosley 2018) can have a major influence on shrimp populations. We attempted to determine the effect of variable recruitment on shrimp density by creating a stochastic recruitment model which took into account the irregular nature of settlement for *N. californiensis*. Model results showed that *N. californiensis* can persist at an average low abundance (~14 shrimp m^{-2}) with generally low, irregular recruitment and high mortality. The stochastic model also showed shrimp densities to increase then steadily decrease similar to observations from previous and current monitoring

678 programs of *N. californiensis* populations (Bird 1982; Dumbauld et al. 1996; Feldman et al.
679 2000; Dumbauld and Bosley, 2018). Our models showed that, theoretically, long-term shrimp
680 abundance would be above the current threshold for implementing shrimp control in Washington
681 State (10 burrows m^{-2}; Dumbauld et al. 2006). This suggests that baseline shrimp abundance
682 would qualify for implementation of control measures, although it is not clear if shrimp cause
683 significant impact to oyster beds at this low density.
684 The persistence of burrowing shrimp populations is clearly linked to the rate at which
685 new animals enter the population and the rate at which they die. Lipofuscin aging has provided
686 evidence that *N. californiensis* is a long-lived animal which explains why populations are stable
687 despite unpredictable recruitment (Chesson and Warner, 1981; Chesson, 1983). However, our
688 model projections showed that temporal patterns of recruitment had a marked effect on overall
689 population density. Settlement strength is a very difficult process to quantify and in many cases
690 settlement does not correlate to recruitment in benthic invertebrates (Fraschetti et al., 2002;
691 Pineda et al., 2010). Assuming that mortality remains constant after juveniles recruit into the
692 adult shrimp population, simple calculations can be used to estimate the abundance of the
693 following year's shrimp population within areas of interest using data on recruitment and
694 population abundance from the current year. These predictions will be useful in guiding
695 management decisions regarding when to control shrimp and where control may be needed, if at
696 all. Future work should consider the development of survey methods to quantify the spatial and
697 temporal distribution of juveniles within and around areas of interest and also tracking shrimp
698 populations on shellfish beds to determine where and when shrimp have a potential to
699 significantly impact shellfish production.
700

5. Conclusions

Our study is the first to apply lipofuscin-based aging methods to estimate mortality and inform a population dynamics model of a shrimp species. Through broad-scale multi-year surveys, we documented changes in the population abundance of *N. californiensis* and established the methodology to explore spatiotemporal variation in abundance of burrowing shrimp in estuarine systems. In addition, our work generates hypotheses regarding burrowing shrimp life-history and elucidates several areas of research that would provide information to further refine our understanding of burrowing shrimp population ecology including, identifying the major causes of adult mortality and quantification of the modes and rates of migration. Finally, the population parameters and cohort model derived in this study can be used to project future shrimp abundance, providing a valuable tool which can be incorporated into decision-making frameworks and used for development of future monitoring plans.

Acknowledgments

This work was funded by the USDA-ARS (CRIS project 5358-63000-002-00D) and the NOAA/SeaGrant Fellowship for Population Dynamics. I would like to thank G. Waldbusser, C. J. Langdon and Lee McCoy for their helpful comments on study design and assistance with manuscript preparation. I also thank Daniel Sund, Natalie Coleman, Drew Hill, Misti Zerbin and other interns that participated in the Research Experience for Undergraduates program at HMSC for their help with data collection and fieldwork. Finally, I would like to thank the anonymous reviewers that provided helpful and constructive comments on this manuscript.

Literature Cited

724 Allain RN, Moriyasu M, Crawford BD, Courtenay SC (2011) Lipofuscin quantification as a
725 potential tool for age estimation in snow crabs, *Chionoecetes opilio* (O. Fabricius, 1788)
726 (Decapoda, Oregoniidae). Crustaceana 84:1441–1463
727
728 Allan EL, Froneman PW, Hodgson AN (2006) Effects of temperature and salinity on the
729 standard metabolic rate (SMR) of the caridean shrimp *Palaemon peringueyi*. J Exp Mar Bio Ecol
730 337:103–108
731
732 Beissinger, SR & McCullough, DR (2002) Population viability analysis Chicago: University of
733 Chicago Press.
734
735 Berkenbusch K, Rowden AA (2003) Ecosystem engineering — moving away from “just so”
736 stories Scaling organisms as ecosystem engineers. N Z J Ecol 27:67–73
737
738 Berkenbusch K, Rowden AA (2006) An examination of the spatial and temporal generality of
739 the influence of ecosystem engineers on the composition of associated assemblages. Aquat Ecol
740 41:129–147
741
742 Berkenbusch K, Rowden AA, Myers TE (2007) Interactions between seagrasses and burrowing
743 ghost shrimps and their influence on infaunal assemblages. J Exp Mar Bio Ecol 341:70–84
744

745 Bertness MD, Grosholz E, Bertness MD, Grosholz E (1985) Population dynamics of the Ribbed
746 Mussel , *Geukensia demissa*: the costs and benefits of an aggregated distribution. Oecologia
747 67:192–204
748
749 Bird E (1982) Population dynamics of thalassinidean shrimps and community effects through
750 sediment modification. PhD thesis, University of Maryland, College Park
751
752 Bivand R, Keitt T, Rowlingson B (2015) rgdal: bindings for the geospatial data abstraction
753 library. R package version 1.1-3. https://CRAN.R-project.org/packge=rgdal
754
755 Bluhm BA, Brey T (2001) Age determination in the Antarctic shrimp *Notocrangon antarcticus*
756 (Crustacean:Decapoda), using the autofluorescent pigment lipofuscin. Mar Biol 138:247–257
757
758 Bluhm BA, Brey T, Klages M (2001) The autofluorescent age pigment lipofuscin: key to age,
759 growth and productivity of the Antarctic amphipod *Waldeckia obesa* (Chevreux, 1905). J Exp
760 Mar Biol Ecol 258:215–235
761
762 Bosley KM (2016) An integrated approach to age, growth and population dynamics of
763 thalassinidean burrowing shrimps in a US west coast estuary. PhD Dissertation, Oregon State
764 University, Corvallis, OR
765
766 Bosley KM, Dumbauld BR (2011) Use of extractable lipofuscin to estimate agestructure of
767 ghost shrimp populations in west coast estuaries of the USA. Mar Ecol Prog Ser 428:161–176

768

769 Brenning A (2012) Spatial cross-validation and bootstrap for the assessment of prediction rules
770 in remote sensing: The R package sperrorest. Int Geosci Remote Sens Symp. pp. 5372–5375

771

772 Caley MJ, Carr MH, Hixon MA, Hughes TP, Menge BA (1996) Recruitment and the local
773 dynamics of open marine populations. Annu Rev Ecol Evol Syst 27:477-500

774

775 Carey JR, Papadopoulos NT, Müller HG, Katsoyannos BI, Kouloussis NA, Wang JL, Wachter
776 K, Yu W, Liedo P (2008) Age structure changes and extraordinary lifespan in wild medfly
777 populations. Aging Cell 7:426–437

778

779 Castorani MCN, Hovel KA, Williams SL, Baskett ML (2014) Disturbance facilitates the
780 coexistence of antagonistic ecosystem engineers in California estuaries. Ecology 95:2277–2288

781

782 Caswell H (2001) Matrix Population Models, Second. Sinauer Associates, Inc, Sunderland, MA

783

784 Chang YJ, Sun CL, Chen Y, Yeh SZ (2012) Modelling the growth of crustacean species. Rev
785 Fish Biol Fish 22:157–187

786

787 Chesson PL (1983) Coexistence of competitors in a stochastic environment: the storage effect.
788 Lect Notes Biomath 52:188–198

789

790 Chesson PL, Warner R (1981) Environmental variability promotes coexistence in lottery
791 competitive systems. Am Nat 117:923–943
792
793 Chew KK (2002) Burrowing shrimp vs. Pacific Northwest Oysters. Aquac Mag 28:71–75
794
795 Cole LC (1954) Population consequences of life-history phenomena. Q Rev Biol 29:131-159
796
797 Commito JA, Celano EA, Celico HJ, Como S, Johnson CP (2005) Mussels matter: Postlarval
798 dispersal dynamics altered by a spatially complex ecosystem engineer. J Exp Mar Bio Ecol
799 316:133–147
800
801 Conides AJ, Nicolaidou A, Apostolopoulou M, Thessalou-legaki M (2012) Growth, mortality
802 and yield of the mudprawn *Upogebia pusilla* (Petagna , 1792) (Crustacea:Decapod:Gebiidea)
803 from western Greece. Acta Adriat 53:87–103
804
805 D'Andrea A, DeWitt TH (2009) Geochemical ecosystem engineering by the mud shrimp
806 *Upogebia pugettensis* (Crustacea:Thalassinidae) in Yaquina Bay, Oregon: Density-dependent
807 effects on organic matter remineralization and nutrient cycling. Limnol Oceanogr 54:1911–1932
808
809 DeWitt TH, D'Andrea AF, Brown CA, Griffen BD, Eldridge PM (2004) Impact of burrowing
810 shrimp populations on nitrogen cycling and water quality in western North American temperate
811 estuaries. In: Proceedings of the symposium on ecology of large bioturbators in tidal flats and

812 shallow sublittoral sediments from individual behavior to their role as ecosystem engineers.
813 Univ. of Nagasaki.
814
815 Du J (2002) Combined algorithms for constrained estimation of finite mixture distributions with
816 grouped data and conditional data. M.S. Thesis, McMaster University. p. 124.
817
818 Dumbauld, BR (1994) Thalassinid shrimp ecology and the use of carbaryl to control populations
819 on oyster ground in Washington coastal estuaries. Ph.D. dissertation, University of Washington,
820 Seattle, Washington. p. 192.
821
822 Dumbauld B, Bosley KM (2018) Recruitment Ecology of Burrowing Shrimps in US Pacific
823 Coast. Estuaries and Coasts 41:1848-1867
824
825 Dumbauld BR, Armstrong DA, Feldman KL (1996) Life-history characteristics of two sympatric
826 thalassinidean shrimps, *Neotrypaea californiensis* and *Upogebia pugettensis*, with implications
827 for oyster culture. J Crustac Biol 16:689–708
828
829 Dumbauld BR, Booth S, Cheney D, Suhrbier A, Beltran H (2006) An integrated pest
830 management program for burrowing shrimp control in oyster aquaculture. Aquaculture 261:976–
831 992
832
833 Fairweather PG (1988) Consequences of Supply-Side Ecology: manipulating the recruitment of
834 intertidal barnacles affects the intensity of predation upon them. Biol Bull 175:349-354

835

836 Feldman KL, Armstrong DA, Dumbauld BR, DeWitt TH, Doty DC (2000) Oysters, crabs, and
837 burrowing shrimp: review of an environmental conflict over aquatic resources and pesticide use
838 in Washington State's (USA) coastal estuaries. Estuaries 23:141-176

839

840 Fraschetti S, Giangrande A, Terlizzi A, Boero F (2002) Pre- and post-settlement events in
841 benthic community dynamics. Oceanol Acta 25:285–295

842

843 Grosberg RK, Levitan DR (1992) For adults only? Supply-side ecology and the history oflarval
844 biology. Trends Ecol Evol 7:130–3

845

846 Hartnoll RG (2001) Growth in Crustacea - Twenty years on. Hydrobiologia 449:111–122

847

848 Harvey HR, Ju S-J, Son S-K, Feinberg LR, Shaw CT, Peterson WT (2010) The biochemical
849 estimation of age in euphausiids: Laboratory calibration and field comparisons. Deep Sea Res
850 Part II Top Stud Oceanogr 57:663–671

851

852 Hewitt JE, Pridmore RD, Thrush SF, Cummings VJ (1997) Assessing the short-term stability of
853 spatial patterns of macrobenthos in a dynamic estuarine system. Limnol Oceanogr 42:282–288

854

855 Hiebenthal C, Philipp E, Eisenhauer A, Wahl M (2012) Interactive effects of temperature and
856 salinity on shell formation and general condition in Baltic Sea *Mytilus edulis* and *Arctica*
857 *islandica*. Aquat Biol 14:289–298

Hijmans RJ, van Etten J (2012) raster: Geographic analysis and modeling with raster data. R package version 2.0-12. http://CRAN.R-project.org/package=raster

Hilborn R, Walters CJ (1992) Quantitative fisheries stock assessment: choice, dynamics, and uncertainty. Chapman and Hall, London

Ju S, Secor DH, Harvey HR (2003) Demographic assessment of the blue crab (*Callinectes sapidus*) in Chesapeake Bay using extractable lipofuscins as age markers. Fishery Bulletin 101:312 - 320

Kincaid TM, Olsen, AR (2015). spsurvey: Spatial survey design and analysis. R package version 3.1. URL: http://www.epa.gov/nheerl/arm/.

Kodama K, Shiraishi H, Morita M, Horiguchi T (2006) Verification of lipofuscin-based crustacean ageing: seasonality of lipofuscin accumulation in the stomatopod *Oratosquilla oratoria* in relation to water temperature. Mar Biol 150:131–140

Kritzer JP, Davies CR, Mapstone BD (2001) Characterizing fish populations: effects of sample size and population structure on the precision of demographic parameter estimates. Can J Fish Aquat Sci 58:1557-1568

880 Kumagai NH (2006) Distance effects on patterns and processes of dispersal in an octocoral
881 amphipod. Mar Ecol Prog Ser 321:203–214
882
883 Lahiri SN, Kaiser MS, Cressie N, Hsu N-J (1999) Prediction of spatial cumulative distribution
884 functions using subsampling. J Am Stat Assoc 94:86–97
885
886 Lahiri SN, Zhu J (2006) Resampling methods for spatial regression models under a class of
887 stochastic designs. Ann Stat 34:1774–1813
888
889 Lenihan HS, Micheli F (2001) Soft-sediment communities. In: Bertness MD, Gaines SD, Hay
890 MH (eds) Marine Community Ecology. Sinauer Associates, Inc, p 253–288
891
892 Leslie, PH (1945) On the use of matrices in certain population mathematics. Biometrika 33: 183-
893 212.
894
895 Lundquist CJ, Thrush SF, Coco G, Hewitt JE (2010) Interactions between disturbance and
896 dispersal reduce persistence thresholds in a benthic community. Mar Ecol Prog Ser 413:217–228
897
898 Macdonald P, Du J (2012) mixdist: finite mixture distribution models. R package version 0.5-4.
899 https://CRAN.R-project.org/package=mixdist
900

McGaffin AF, Nicol S, Virtue P, Hirano Y, Matsuda T, Uchida I, Candy SG, Kawaguchi S (2011) Validation and quantification of extractable age pigments for determining the age of Antarctic krill (*Euphausia superba*). Mar Biol 158:1743-1755

Menge BA., Chan F, Nielsen KJ, Lorenzo E Di, Lubchenco J (2009) Climatic variation alters supply-side ecology: Impact of climate patterns on phytoplankton and mussel recruitment. Ecol Monogr 79:379–395

Menge BA., Gouhier TC, Freidenburg T, Lubchenco J (2011) Linking long-term, large-scale climatic and environmental variability to patterns of marine invertebrate recruitment: toward explaining "unexplained" variation. J Exp Mar Bio Ecol 400:236–249

Minchinton TE (1997) Life on the edge: conspecific attraction and recruitment of populations to disturbed habitats. Oecologia 111:45–52

Morris WF, Doak DF (2002) Quantitative conservation biology. Sinauer Associates, Inc, Sunderland, MA

Morrisey DJ, Underwood AJ, Howitt L, Stark JS (1992) Temporal variation in soft sediment benthos. J Exp Mar Bio Ecol 164:233–245

Newman, MD (1993) Regression analysis of log-transformed data: Statistical bias and its correction. Environ Toxicol Chem 12:1129–1133

924

925 Nilssen EM, Sundet JH (2006) The introduced species red king crab (*Paralithodes*
926 *camtschaticus*) in the Barents Sea. II. Growth increments and moulting probability. Fish Res
927 82:319–326
928 Northern Economics, Inc. The Economic Impact of Shellfish Aquaculture in Washington,
929 Oregon and California. Prepared for Pacific Shellfish Institute. April 2013.
930
931 O'Donovan V, Tully O (1996) Lipofuscin (age pigment) as an index of crustacean age:
932 correlation with age, temperature and body size in cultured juvenile *Homarus gammarus* L . J
933 Exp Mar Bio Ecol 207:1–14
934
935 Oh C, Hartnoll RG (2000) Effects of food supply on the growth and survival of the common
936 shrimp, *Crangon crangon* (Linnaeus, 1758) (Decapoda, Caridea). Crustaceana 73:83–99
937
938 Ohman MD (2012) Estimation of mortality for stage-structured zooplankton populations: What
939 is to be done? J Mar Syst 93:4–10
940
941 Olaffsson EB (1994) Does recruitment limitation structure populations and communities of
942 macro-invertebrate marine soft-sediments: The relative significance of pre- and post-settlement
943 processes. Oceanogr Mar Biol Annu Rev 32:171–179
944

945 Pacheco AS, Uribe RA, Thiel M, Oliva ME, Riascos JM (2013) Dispersal of post-larval
946 macrobenthos in subtidal sedimentary habitats: Roles of vertical diel migration, water column,
947 bedload transport and biological traits' expression. J Sea Res 77:79–92
948
949 Peterson CH (1984) Does a rigorous criterion for environmental identity preclude the existence
950 of multiple stable points? Am Nat 124:127–133
951
952 Pineda J, Porri F, Starczak V, Blythe J (2010) Causes of decoupling between larval supply and
953 settlement and consequences for understanding recruitment and population connectivity. J Exp
954 Mar Bio Ecol 392:9–21
955
956 Pezzuto, PR (1998) Population dynamics of *Sergio mirim* (Rodrigues 1971) (Decapoda:
957 Thalassinidea: Callianassidae) in Cassino Beach, southern Brazil. Mar Ecol PSZNI 19:89-109
958
959 Posey MH (1986) Changes in a benthic community associated with dense beds of a burrowing
960 deposit feeder, *Callianassa californiensis*. Mar Ecol 31:15–22
961
962 Puckett BJ, Secor DH, Ju S-J (2008) Validation and application of lipofuscin-based age
963 determination for Chesapeake Bay blue crabs *Callinectes sapidus*. Trans Am Fish Soc
964 137:1637–1649
965 Punt AE, Huang T, Maunder MN (2014) Review of integrated size-structured models for stock
966 assessments of hard-to-age crustacean and mollusc species. ICES J Mar Sci 70:16-33
967

968 R Core Development Team (2016) R: A language and environment for statistical computing. R
969 Foundation for Statistical Computing, Vienna, Austria. URL http://www.R-project.org/.
970
971 Robson D., Chapman D (1961) Catch curves and mortality rates. Trans Am Fish Soc 90:312-322
972
973 Rosenberg R (1974) Spatial dispersion of an estuarine benthic faunal community. J Exp Mar Bio
974 Ecol 15:69–80
975
976 Shanks AL, Roegner GC (2007) Recruitment limitation in dungeness crab populations is driven
977 by variation in atmospheric forcing. Ecology 88:1726–1737
978
979 Sheehy MRJ, Greenwood JG, Fielder DR (1995) lipofuscin as a record of "rate of living" in an
980 aquatic poikilotherm. J Geronology 50:327–336
981
982 Stoner AW, Copeman LA, Ottmar ML (2013) Molting, growth, and energetics of newly settled
983 blue king crab: effects of temperature and comparisons with red king crab. J Exp Mar Bio Ecol
984 442:10–21
985
986 Tamaki A, Ingole B (1993) distribution of juvenile and adult ghost shrimps, *Callianassa*
987 *japonica* Ortmann (Thalassinidea), on an intertidal sand flat: intraspecific facilitation as a
988 possible pattern-generating factor. J Crustac Biol 13:175–183
989

990 Tamaki A, Ingole B, Ikebe K, Muramatsu K, Taka M, Tanaka M (1997) Life history of the ghost
991 shrimp, *Callianassa japonica* Ortmann (Decapoda:Thalassinidea), on an intertidal sandflat in
992 western Kyushu, Japan. J Exp Mar Bio Ecol 210:223–250
993
994 Tamaki A, Mandal S, Agata Y, Aoki I, Suzuki T, Kanehara H, Aoshima T, Fukuda Y,
995 Tsukamoto H, Yanagi T (2010) Complex vertical migration of larvae of the ghost shrimp,
996 *Nihonotrypaea harmandi*, in inner shelf waters of western Kyushu, Japan. Estuar Coast Shelf Sci
997 86:125–136
998
999 Terman A (2001) Garbage catastrophe theory of aging: imperfect removal of oxidative damage?
1000 Redox Rep 6:15–26
1001
1002 Thrush SF (1991) Spatial patterns in soft-bottom communities. Trends Ecol Evol 6:75–79
1003
1004 Tomczak M (1998) Spatial interpolation and its uncertainty using automated anisotropic inverse
1005 distance weighting (IDW) - cross-validation/jackknife approach. J Geogr Inf Decis Anal 2:18–30
1006
1007 Udevitz M, Ballachey B (1998) Estimating survival rates with age-structure data. J Wildl
1008 Manage 62:779–792
1009
1010 Udevitz MS, Gogan PJP (2012) Estimating survival rates with time series of standing age-
1011 structure data. Ecology 93:726–732
1012

1013 Underwood AJ, Fairweather PG (1989) Supply-side ecology and benthic marine assemblages.
1014 Trends Ecol Evol 4:16–20
1015
1016 USDA NASS, 2012 Census of Agriculture, Ag Census Web Maps. Available at:
1017 www.agcensus.usda.gov/Publications/2012/Online_Resources/Ag_Census_Web_Maps/Overvie
1018 w/.
1019
1020 Valanko S, Norkko A, Norkko J (2010) Strategies of post-larval dispersal in non-tidal soft
1021 sediment communities. J Exp Mar Bio Ecol 384:51–60
1022
1023 Vila Y, Medina A, Megina C, Ramos F, Sobrino I (2000) quantification of the age pigment
1024 lipofuscin in brains of known-age, pond-reared prawns *Penaeus japonicus* (Crustacea,
1025 Decapoda). 268:120–130
1026
1027 Washington Department of Fisheries and Wildlife (1970) Ghost shrimp control experiments with
1028 Sevin, 1960–1968. Washington Department of Fisheries Technical Report, vol.1, p1–62
1029
1030 Washington Department of Fisheries and Wildlife, Washington Department of Ecology (1992)
1031 Use of the insecticide carbaryl to control ghost and mud shrimp in oyster beds of Willapa Bay
1032 and Grays Harbor. Final Supplemental Environmental Impact Statement, Olympia, Washington.
1033 p. 197
1034

1035 Whitlatch RB, Lohrer AM, Thrush SF, Pridmore RD, Hewitt JE, Cummings VJ, Zajac RN
1036 (1998) Recruitment, colonization and physical-chemical forcing in marine biological systems:
1037 proceedings of the 32nd European marine biology symposium, held in Lysekil, Sweden, 16-22
1038 August 1997. In: Baden S, Phil L, Rosenberg R, Strömberg J-O, Svane I, Tiselius P (eds)
1039 Springer Netherlands, Dordrecht, p 217–226
1040
1041 Woodin SA (1976) Adult-larval interactions in dense infaunal assemblages: patterns of
1042 abundance. J Mar Res 34:25–41
1043
1044 Woodson CB, McManus MA., Tyburczy JA., Barth JA., Washburn L, Caselle JE, Carr MH,
1045 Malone DP, Raimondi PT, Menge BA., Palumbi SR (2012) Coastal fronts set recruitment and
1046 connectivity patterns across multiple taxa. Limnol Oceanogr 57:582-596
1047

Population Assessments

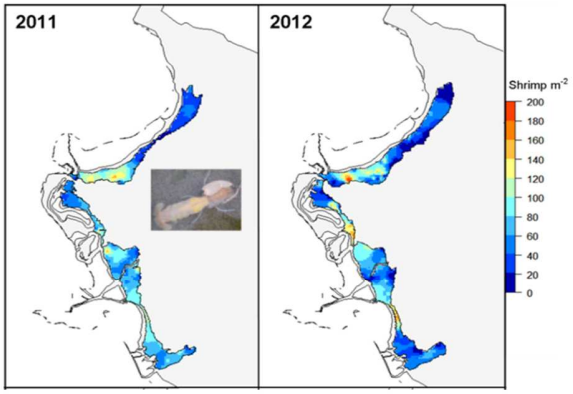

Mortality Estimation

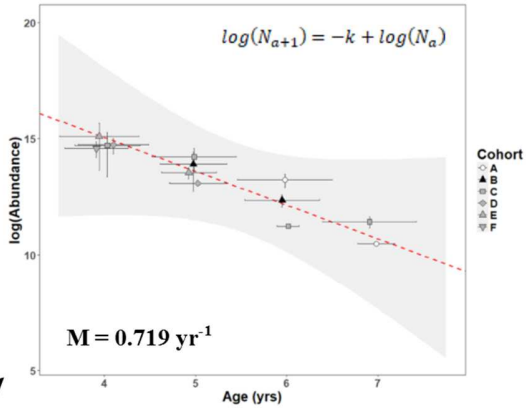

Lipofuscin-Based Age Structure

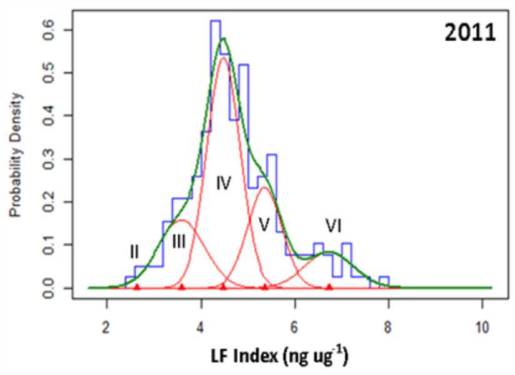

Population Scenarios